Visco-elastic behavior of polymers

4.1.2 Material Behavior and Constitutive Equations

The relationship between the mechanical loading parameters stress and strain is determined by material behavior and described by constitutive equations. It occurs in an enormous variety of combinations depending on the structural state of the investigated material, as well as the loading conditions. In the area of polymers alone, its spectrum ranges from brittle glassy solidified amorphous polymers to ductile semicrystalline thermoplastics to soft elastomers all the way to fluid-like polymer melts. Due to the multiplicity of observable phenomena, a uniform description is scarcely possible. Instead, basic types of mechanical behavior are defined using simplified assumptions that allow us to approximate a description of the stress–strain relationship within a narrow range of validity.

4.1.2.1 Elastic Behavior

The mechanical behavior of a material is called elastic as long as there is a bijective relationship between its stress and deformation states, i.e., entirely reversible in the mechanical as well as thermodynamic sense. With respect to different thermodynamic causes, we distinguish between energy elasticity and entropy elasticity.

Energy Elasticity

The structural cause of energy-elastic behavior is a change in median interatomic distances and bond angles under the influence of mechanical loading. The required mechanical work is stored in the form of potential energy (increase in internal energy) and entirely regained when loading is removed (first law of thermodynamics). Due to its structural causes, energy-elastic behavior remains limited to relatively small deformations. Here we can observe a linear relationship

between stress and strain as described by *Hooke*'s law. In a simple case of uniaxial tensile loading (see Fig. 4.1a), it holds that:

$$\sigma = E \cdot \varepsilon \tag{4.12}$$

The proportionality constant between stress and strain is called the modulus of elasticity *E*. It is related to the bonding forces in the material. Alternatively, compliance *C* can also be determined:

$$\varepsilon = C \cdot \sigma \tag{4.13}$$

In addition to length change, a tensile loaded specimen simultaneously undergoes reduction in cross-section. The magnitude of this cross-sectional change is described by *Poisson*'s ratio *ν*. It expresses the relationship between strains in the latitudinal (ε_y, ε_z) and longitudinal (ε_x) directions. In cases of uniaxial loading, it holds that:

$$\nu = -\frac{\varepsilon_y}{\varepsilon_x} = -\frac{\varepsilon_z}{\varepsilon_x} \tag{4.14}$$

For the general case of multiaxial loading, energy-elastic behavior is described by the generalized *Hooke*'s law. It is based on the assumption that each of the six components of the stress tensor σ_{ij} is linear-dependent on the six components of the deformation tensor ε_{kl}:

$$\boldsymbol{\sigma_{ij}} = C_{ijkl} \cdot \boldsymbol{\varepsilon_{kl}} \tag{4.15}$$

$$\boldsymbol{\varepsilon_{ij}} = D_{ijkl} \cdot \boldsymbol{\sigma_{kl}} \tag{4.16}$$

The proportionality constants between the components of the stress and deformation tensors form a forth order tensor, also called the elasticity tensor C_{ijkl} or compliance tensor D_{ijkl}. This tensor consists of 81 components of which, however, only 21 are independent of one another in static equilibrium. Symmetry properties of the material can lead to a further reduction in the number of independent components. Two components are required in order to completely describe the elasticity and/or compliance tensor of an isotropic material. The relationship between stress and deformation state of an isotropic material can be vectorially expressed as follows [4.4]:

$$\begin{Bmatrix} \sigma_{xx} \\ \sigma_{yy} \\ \sigma_{zz} \\ \tau_{xy} \\ \tau_{yz} \\ \tau_{zx} \end{Bmatrix} = \begin{bmatrix} C_{11} & C_{12} & C_{12} & 0 & 0 & 0 \\ C_{12} & C_{11} & C_{12} & 0 & 0 & 0 \\ C_{12} & C_{12} & C_{11} & 0 & 0 & 0 \\ 0 & 0 & 0 & \frac{C_{11}-C_{12}}{2} & 0 & 0 \\ 0 & 0 & 0 & 0 & \frac{C_{11}-C_{12}}{2} & 0 \\ 0 & 0 & 0 & 0 & 0 & \frac{C_{11}-C_{12}}{2} \end{bmatrix} \cdot \begin{Bmatrix} \varepsilon_{xx} \\ \varepsilon_{yy} \\ \varepsilon_{zz} \\ \gamma_{xy} \\ \gamma_{yz} \\ \gamma_{zx} \end{Bmatrix} \tag{4.17}$$

The elastic constants C_{11} and C_{12} stand in relation to the modulus of elasticity E and *Poisson*'s ratio ν of an isotropic material:

$$C_{11} = \frac{E(1-\nu)}{(1+\nu)(1-2\nu)} \tag{4.18}$$

$$C_{12} = \frac{E\nu}{(1+\nu)(1-2\nu)} \tag{4.19}$$

From the modulus of elasticity E and *Poisson*'s ratio ν, further material parameters can be calculated such as shear modulus G and compression modulus K:

$$G = \frac{\tau}{\gamma} = \frac{E}{2(1+\nu)} = \frac{C_{11}-C_{12}}{2} \tag{4.20}$$

$$K = \frac{p}{\Delta V/V_0} = \frac{E}{3(1-2\nu)} = \frac{C_{11}+2C_{12}}{3} \tag{4.21}$$

Energy elasticity dominates the behavior of polymer materials for relatively small deformations, especially at low temperatures and high loading rates. Here, energy elasticity theory contributes strongly to our understanding of the deformation behavior. Moreover, it provides workable approximating solutions for a quantitative description of the stress–strain relationship.

Entropy Elasticity

By entropy elasticity we mean the tendency of macromolecules to return to their entropically most advantageous, i.e., coiled, state subsequent to deformation. If a flexible-chained polymer material is subjected to mechanical loading, its macromolecules orientate in the stress field. The state of molecular order is accompanied by a reduction in system entropy. If irreversible chain slip can be prevented, for example by crosslinking, the molecules tend to maximize entropy

upon being released (second law of thermodynamics). They assume a permanent unordered state of equilibrium.

Entropy-elastic behavior up to strains of several hundred percent can be observed, whereby the relationship between stress and deformation is non-linear. Simple continuum mechanical considerations, as well as molecular statistical models [4.5] in the case of uniaxial load, lead to the following relation:

$$\sigma = \frac{E}{3} \cdot (\lambda - \lambda^{-2}) \tag{4.22}$$

The material's parameter modulus of elasticity E is determined by the crosslink density N or average molecular weight between the crosslinking points of the polymer M_C. Moreover, it is dependent on temperature T as well as on the *Boltzmann* number k or the universal gas constant R and density ρ:

$$E = 3NkT = \frac{3\rho}{M_C} RT \tag{4.23}$$

Using Eq. 4.22, essential phenomena of mechanical behavior of vulcanized rubber can be illustrated. Their quantitative validity often remains limited to strains of less than 100 %. For this reason, the simple rubber elasticity theory has undergone a series of further developments which are covered in [4.6], for example.

Entropy elasticity is not limited to covalent crosslinked polymers. It also plays an important role above the glass transition temperature in amorphous and semicrystalline thermoplastics of sufficiently high molecular weight. Here, molecular entanglements assume the role of temporary crosslinking points [4.7 – 4.9].

4.1.2.2 Viscous Behavior

In contrast to elastic behavior, viscous behavior is characterized by the total irreversibility of deformation processes. Therefore,

1. Once deformation has been effected, it remains in place even after unloading; the relationship between stress and strain is unambiguous only with respect to prehistory; however, it is no unique reversible relationship.
2. Work expended on deformation is entirely dissipated by the material.

Structurally speaking, viscous behavior is characterized by relative displacement among adjacent structure units (molecules and/or molecule sequences in polymer materials). Any frictional forces to be overcome are dependent on deformation velocity. When the relationship observed between stress and deformation velocity is

linear, we speak of *Newtonian* material behavior. This is characterized by the material parameter viscosity η. In cases of simple shear loading (shear flow) it holds that:

$$\tau = \eta \cdot \frac{d\gamma}{dt} = \eta \cdot \dot{\gamma} \tag{4.24}$$

By analogy in cases of elongational flow under normal stress loading, it holds that:

$$\sigma = \eta^T \cdot \frac{d\varepsilon}{dt} = \eta^T \cdot \dot{\varepsilon} \tag{4.25}$$

The viscosity η^T is called elongational viscosity or *Trouton* viscosity. At low shear rates, it is three times greater than shear viscosity η (*Trouton* ratio $\eta^T/\eta = 3$) [4.10].

Newtonian behavior is found in polymer melts. Here, however, it is generally limited to low shear rates. At higher shear rates, shear softening, also called pseudoplasticity, often occurs . More rarely observed is shear hardening (dilatancy). As it deviates from *Newtonian* behavior, viscosity becomes a function of deformation rate. Various rheological methods are available to describe the occurring non-linearities [4.10].

A viscosity theory focusing on structural consideration has been developed by *Eyring* [4.11] (Rate Theory). It describes the irreversible deformation process resulting from local interchange of sites by stress-aided thermal activation. The relationship between shear rate $\dot{\gamma}$ and shear stress τ depends on the characteristic material parameters of the energy barrier height to be overcome during site change (activation enthalpy ΔH_0), the activation volume v and a pre-exponential factor $\dot{\gamma}_0$, as well as on the *Boltzmann* number k and temperature T. This relationship can be expressed as:

$$\dot{\gamma} = \dot{\gamma}_0 \exp\left(-\frac{\Delta H_0}{kT}\right) \sinh\left(\frac{v\tau}{kT}\right) \tag{4.26}$$

To overcome potential barriers in polymer melts, the proportion of mechanical energy is generally small compared to that of thermal energy ($v\tau << kT$). Thereby Eq. 4.26 becomes a borderline case of *Newtonian* behavior ($\dot{\gamma} \sim \tau$). By analogy with Eq. 4.24, the resulting viscosity is:

$$\eta = \eta_0 \exp\left(\frac{\Delta H_0}{kT}\right) \tag{4.27}$$

with

$$\eta_0 = \frac{k\,T}{\dot{\gamma}_0\,v} \tag{4.28}$$

Equation 4.27 describes the temperature dependence of viscosity in the form of an *Arrhenius* relationship. A relationship of this type has been demonstrated in experiments with melts of semicrystalline thermoplastic (far from glass transition temperature). For amorphous polymer melts near glass transition temperature, it is often more advantageous to use the *Vogel/Fulcher/Tammann* equation (Eq. 4.29) which is related to the free volume theory with the constants A and B as well as temperature T_0^{∞} [1.16].

$$\eta = A \exp\left(\frac{B}{T - T_0^{\infty}}\right) \tag{4.29}$$

4.1.2.3 Viscoelastic Behavior

Viscosity and elasticity are the characteristic properties of fluids and solid bodies in the area of low-molecular materials. For polymers they represent merely the limits of a broad spectrum of properties that are characterized by the simultaneous occurrence of viscous and elastic effects called viscoelasticity. The characteristic feature of viscoelastic behavior is the time dependence of material properties. This is expressed, for example, by relaxation and retardation phenomena under static loading. A detailed presentation and interpretation of viscoelastic properties of polymers can be found in the works of *Ferry* [4.12] or *Aklonis* and *MacKnight* [4.13].

Linear Viscoelasticity

When material properties depend only on time, but not on the level of mechanical loading, the material's behavior is called linear-viscoelastic. Linear viscoelasticity is exactly defined only for the range of infinitesimally small loads. In practice, the validity for solid polymers is limited to strains less than 1 %, but for polymer melts it can reach 100 % [4.14].

Linear-viscoelastic behavior can be expressed by a combination of linear-elastic and linear-viscous processes (laws of *Hooke* and *Newton*). Mechanical models can be used for illustration, in which elastic behavior is symbolized by a spring and viscous behavior by a dashpot. In the simplest case, both basic elements are arranged either in series or parallel, as shown in Fig. 4.4.

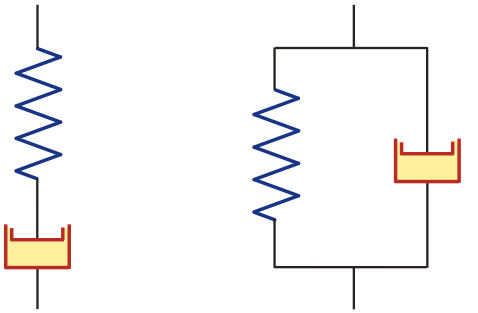

Fig. 4.4: Analogy model for describing viscoelastic behavior

The spring and dashpot series is called the *Maxwell* model. It describes the phenomenon of stress relaxation (reaction to a sudden change of deformation). One characteristic of this model is the additivity of elastic and viscous deformation segments:

$$\varepsilon = \varepsilon_e + \varepsilon_v \tag{4.30}$$

By substituting Eq. 4.12 and 4.25 in Eq. 4.30, we obtain differential equation Eq.4.31. Its solution in the case of stress relaxation ($\dot{\varepsilon} = 0$) results in a temporally exponentially falling stress $\sigma(t)$ (Eq. 4.32), or as a material function in a temporally exponentially falling relaxation modulus $E(t)$ (Eq. 4.33).

$$\dot{\varepsilon} = \frac{1}{E}\dot{\sigma} + \frac{1}{\eta}\sigma \tag{4.31}$$

$$\sigma(t) = \sigma_0 \exp\left(-\frac{E}{\eta^T}t\right) = \sigma_0 \exp\left(-\frac{t}{\tau}\right) \tag{4.32}$$

$$E(t) = \frac{\sigma(t)}{\varepsilon_0} = \frac{\sigma_0}{\varepsilon_0}\exp\left(-\frac{E}{\eta}t\right) = \frac{\sigma_0}{\varepsilon_0}\exp\left(-\frac{t}{\tau}\right) \tag{4.33}$$

The quotient η/E represents the model time constant, also called relaxation time τ. Once a relaxation time has to be considered, the *Maxwell* model is incapable of describing the complex relaxation behavior of real polymers. Correspondence between model and experiment can be achieved by introducing a discrete relaxation time spectrum. This can be illustrated in the analogy model by several *Maxwell* elements arranged in parallel, as is shown in Fig. 4.5.

The relaxation modulus $E(t)$ of this generalized *Maxwell* model results from the sum of individual relaxation moduli $E_i(t)$:

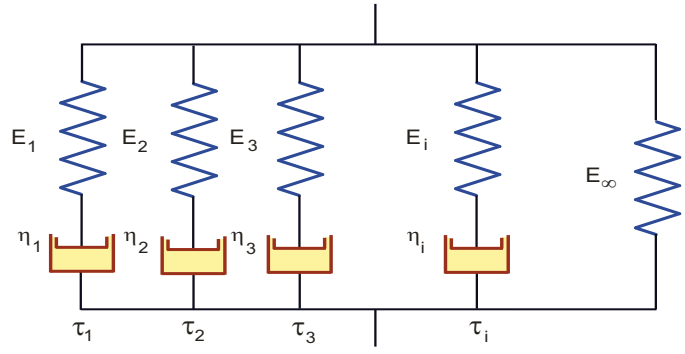

Fig. 4.5: Generalized *Maxwell* model

$$E(t) = E_\infty + \sum_{i=1}^{n} E_i \exp\left(-\frac{t}{\tau}\right) \tag{4.34}$$

As $n \to \infty$, transition takes place to a continuous relaxation time spectrum $H(\tau)$:

$$E(t) = E_\infty + \int_{-\infty}^{+\infty} H(\tau) \exp\left(-\frac{t}{\tau}\right) d(\ln \tau) \tag{4.35}$$

In contrast to the *Maxwell* model, the parallel arrangement of spring and dashpot known as the *Voigt-Kelvin* model characterizes retardation behavior (reaction to a sudden change of stress). Analogous to the procedure described above, compliance $C(t)$ can be calculated as a characteristic value function.

$$C(t) = \frac{\varepsilon(t)}{\sigma_0} = \frac{\varepsilon_0}{\sigma_0}\left[1 - \exp\left(-\frac{t}{\tau}\right)\right] \tag{4.36}$$

Introduction of the retardation time spectrum $L(\tau)$ results in:

$$C(t) = J_\infty + \int_{-\infty}^{+\infty} L(\tau)\left[1 - \exp\left(-\frac{t}{\tau}\right)\right] d(\ln \tau) \tag{4.37}$$

Besides the *Maxwell* and *Voigt-Kelvin* models, rheology uses numerous other rheological models to describe linear-viscoelastic behavior. Regardless of the approach used, its mathematical description leads to a linear differential equation with the form

$$\begin{aligned} &a_0\varepsilon + a_1\dot{\varepsilon} + a_2\ddot{\varepsilon} + a_3\dddot{\varepsilon} + \ldots = b_0\sigma + b_1\dot{\sigma} + b_2\ddot{\sigma} + b_3\dddot{\sigma} + \ldots \\ &a_i, b_i = \text{const} \end{aligned} \tag{4.38}$$

which forms the basis for linear viscoelasticity theory. It is the theoretical foundation for a series of rules whose applicability has contributed to the acceptance of the theory.

Boltzmann Superposition Principle

The *Boltzmann* superposition principle describes the influence of mechanical prehistory on material behavior. It states that the time-dependent effects of sequential changes in the loading state combine linearly to the overall effect. Figure 4.6 illustrates this with a creep recovery experiment.

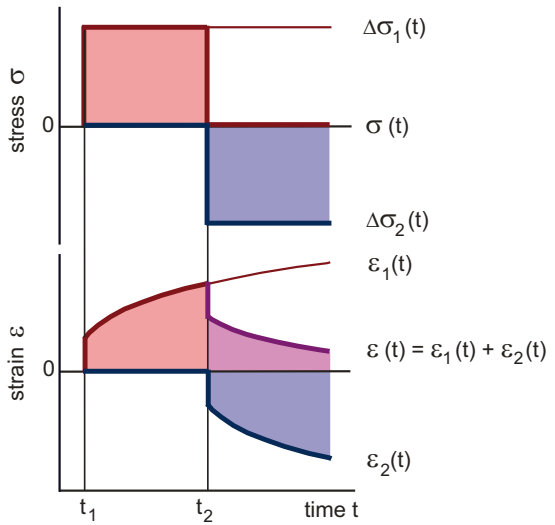

Fig. 4.6: Linear overlapping of strains $\varepsilon_1(t)$ and $\varepsilon_2(t)$ occurring as a result of sudden stress changes $\Delta\sigma_1$ and $\Delta\sigma_2$ using a creep recovery experiment as an example

At time t_1, stress change $\Delta\sigma_1$ is generated, effecting a time-dependent deformation change $\varepsilon_1(t)$. Any further stress change $\Delta\sigma_2 = -\Delta\sigma_1$ at time t_2 has the same effect. However, $\varepsilon_2(t)$ lags behind and has an opposite direction. The total effect $\varepsilon(t)$ of sequential stress changes results from the sum of individual effects $\varepsilon_1(t) + \varepsilon_2(t)$. For n stress steps, it holds that:

$$\varepsilon(t) = \sum_{i=1}^{n} \varepsilon(t - t_i) = \sum_{i=1}^{n} C(t - t_i)\Delta\sigma_i \tag{4.39}$$

From this and by transition to differentially small load changes, the *Boltzmann* superposition integral results

$$\varepsilon(t) = \int_{\tau=-\infty}^{t} C(t-\tau)\frac{d\sigma}{d\tau}\,d\tau \tag{4.40}$$

or

$$\sigma(t) = \int_{\tau=-\infty}^{t} E(t-\tau)\frac{d\varepsilon}{d\tau}d\tau \tag{4.41}$$

which describes the behavior for any given loading history and which can be regarded as a constitutive equation for linear-viscoelastic materials.

Time–Temperature Superposition Principle

Viscoelastic material properties exhibit strong temperature dependence in addition to their pronounced time dependence, because molecular motion and transformation processes determine the relaxation and/or retardation spectrum of the material. These molecular processes are thermally activated and proceed more rapidly as temperature increases. During the process, the relaxation and retardation time spectrum shifts to shorter times. If, in dependence on temperature, only the speed, but not the type or number of molecular processes changes, the relaxation and/or retardation spectrum is maintained, and along with it, the shape of viscoelastic functions along the logarithmic time axis. Their temporal position, however, changes in accordance with the temperature. Such behavior is usually defined as thermorheologically simple. As a consequence of this behavior time-temperature equivalence, applied as a time-temperature superposition principle, has gained great practical significance for predicting long-term behavior. If the progression of a viscoelastic parameter, e.g., modulus *E(log t)*, is known for a certain time interval at varying temperatures, then individual curves, such as in Fig. 4.7, can be horizontally shifted to coincide with curve $E_0(\log t)$ acquired at reference temperature T_0. The

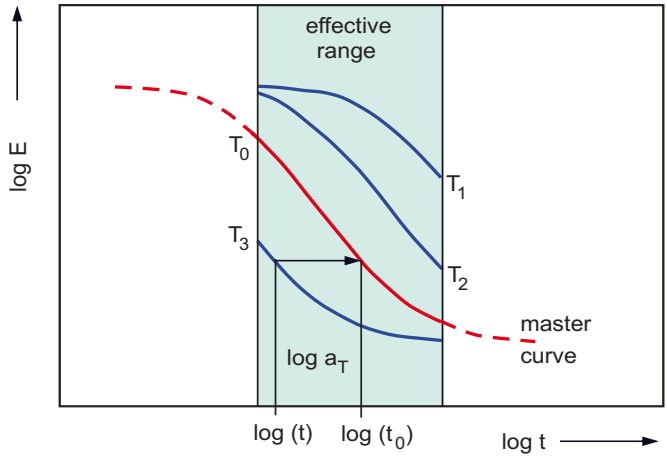

Fig. 4.7: Master curve drawn using time-temperature superposition (diagram)

result is a master curve illustrating material behavior over a wide time range. The shift function $log\ a_T = log\ t - log\ t_0$ is temperature-dependent. In many cases it can be described using an *Arrhenius* approach:

$$\log a_T = \log\left(\frac{t}{t_0}\right) = \frac{\Delta H}{2.3k}\left(\frac{1}{T} - \frac{1}{T_0}\right) \tag{4.42}$$

In the glass transition temperature range, however, it often follows the *Williams/Landel/Ferry* (WLF) equation:

$$\log a_T = \log\left(\frac{t}{t_0}\right) = -\frac{C_1(T - T_0)}{C_2 + T - T_0} \tag{4.43}$$

with universal constants C_1 and C_2 [4.15].

Correspondence Principle

Practical work with linear-viscoelastic constitutive equations can be considerably simplified using *Laplace*'s transformation. That means that a function *y(t)* is transformed into a function $\bar{y}$ with the new variable *s* according to the following rule:

$$\bar{y} = \int_0^\infty y \exp(-st)dt \tag{4.44}$$

If, for example, this procedure is applied to *Boltzmann*'s superposition integral (Eq. 4.41) it results in:

$$\bar{\sigma} = s\bar{E}(s)\bar{\varepsilon} \tag{4.45}$$

Formally this corresponds to *Hooke*'s law (Eq. 4.12), by analogy with which Eq. 4.45 can be modified according to normal rules of algebra, thus leading to the results known from linear elasticity theory. After inverse transformation, it provides a solution to the loading problem for viscoelastic material behavior.

Non-Linear Viscoelasticity

Once the limit of validity of linear viscoelasticity is exceeded, the time and temperature-dependent viscoelastic properties are additionally influenced by load magnitude. Therefore, mechanical behavior can now no longer be described in the form of a linear differential equation. Because the solution of the resulting non-linear differential equations is mathematically extremely complicated and cannot be solved without simplifications, it did not become standard practice. For simple applications,

the *Leadermann* approach [4.16] has often proved satisfactory. It supplements the *Boltzmann* superposition integral (Eq. 4.41) with the load-dependent empirical function $f(\varepsilon)$.

$$\sigma(t) = \int_{\tau=-\infty}^{t} E(t-\tau)\frac{df(\varepsilon)}{d\tau}d\tau \tag{4.46}$$

For stress relaxation as an example, it results in:

$$\sigma(t) = E(t)f(\varepsilon) \tag{4.47}$$

In addition to the procedure described by *Leadermann*, the literature provides numerous additional mathematical approaches for treating non-linear viscoelastic problems [4.10]. Since the introduction of *Fourier* transform rheology, considerable progress has been made in describing non-linear viscoelastic behavior under oscillating loading [4.17].

4.1.2.4 Plastic Behavior

Similar to viscoelastic behavior, a combination of reversible and irreversible processes characterizes plastic behavior. However, in contrast to viscoelastic behavior, they do not occur simultaneously, but are separated from each other by a yield point σ_F. Below the yield point, material behavior is elastic; above it irreversible flow processes take place (see Fig. 4.8a). Using the equations of *Hooke* (Eq. 4.12) and *Newton* (Eq. 4.25), the stress–strain relationship can be formulated as follows:

$$\begin{aligned} \sigma &= E\,\varepsilon && \text{for} \quad \sigma < \sigma_F \\ \sigma &= \eta^T\,\dot{\varepsilon} + \sigma_F && \text{for} \quad \sigma \geq \sigma_F \end{aligned} \tag{4.48}$$

Plastic deformation behavior is detected in many amorphous and semicrystalline polymers. Under uniaxial tensile loading, as illustrated in Fig. 4.8b, it takes the form of yield stress σ_s, characterized by a local maximum in the stress–strain curve and usually observed for elongations ranging from 5 to 25 %.

Instances of yield strain are accompanied by reduction in local cross-section of the specimen also known as necking. In the necking zone, irreversible deformations of several hundred percent occur. Due to this inhomogeneity, considerable discrepancies arise between nominal and true stress and/or strain. By establishing true stress–strain diagrams, it could be shown that the stress reduction after yield stress has been exceeded often is only an apparent geometry effect [4.18].

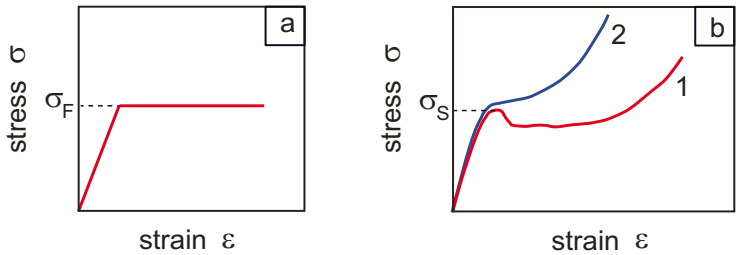

Fig. 4.8: Relationship between stress and strain in plastic material behavior: Model (a) and polymer material (b) (1: nominal (engineering) stress–strain curve; 2: (true stress–strain curve)

The level of yield stress required for plastic flow processes to start depends on the stress state as well as on temperature and loading rate. The influence of stress state can generally be described by the yield criteria of classical mechanics [4.19]. The temperature and velocity dependence of yield flow allows for the thermally active nature of the underlying deformation processes. For amorphous as well as semicrystalline polymers, it often conforms to the *Eyring* equation (Eq. 4.26). With respect to the occuring deformation mechanisms, however, amorphous and semicrystalline polymers exhibit considerable differences. In amorphous polymers, plastic deformation occurs in the glassy state where local molecular motion under the effect of stress forms plasticized microdomains whose growth and conjunction on the macroscopic scale lead to plastic deformation in the form of shear bands or crazes. [4.20, 4.21]. In semicrystalline polymers, plastic deformation generally occurs above the glass temperature of the amorphous phase. Here, crystallographic slip processes represent the decisive step in deformation [4.22 – 4.24] as a result of which the lamellar structure is transformed into a fibrillar structure [4.25, 4.26]. Observation of the deformation mechanisms makes clear that the microscopic processes leading to plastic deformation begin to occur far below the yield point. They can often be identified as early as during loading in the linear-viscoelastic range, so that relationships can be established between relaxation time spectrum and plastic behavior [4.27].

An orientation of the macromolecules takes place as a result of plastic deformation. The achievable changes in properties are the focus of numerous polymer processing technologies. Due to molecular orientation, entropy-elastic restoring forces are triggered that resist plastic deformation and cause strain hardening that are observed with large deformations. If loading is increased further, breaking occurs in overloaded polymer chains, preceding the macroscopic fracture of the material.

4.2 Mechanical Spectroscopy

One characteristic feature of polymer materials is the pronounced time dependence of their mechanical properties. This is caused by the different relaxation times of a wide spectrum of molecular relaxation processes. The relationship between relaxation time spectrum $H(\tau)$ and modulus of elasticity $E(t)$ can be established on the basis of linear viscoelasticity theory using Eq. 4.35. For the sake of simplicity, *Alfery's* approximation solution [4.28] can often be used:

$$H(\tau) = \left.\frac{dE(t)}{d\ln t}\right|_{t=\tau} \tag{4.49}$$

The determination and analysis of the relaxation time spectrum on the basis of mechanical investigations is the subject of mechanical spectroscopy. More specifically, a type of absorption spectroscopy is involved that determines the energy-absorption in the material due to internal friction as a function of the frequency and duration of mechanical loading. The position of an absorption process on the frequency or time axis, as well as its intensity, provides information on the type of underlaying molecular rearrangement as well as on the magnitude and number of structural elements involved. Thus, mechanical spectroscopy is an effective tool for characterizing the structure and explaining molecular relaxation processes.

4.2.1 Experimental Determination of Time Dependent Mechanical Properties

Mechanical spectroscopy is primarily oriented to investigations involving small loads where there is no irreversible structural change in the material, and linear viscoelasticity theory is valid. It is based on experimental data acquirable within a time span of approx. 10^{-8} s to 10^{8} s. A combination of various testing methods is required to characterize mechanical behavior over such a wide time span. For long-term loading times lasting more than a minute, static test methods (stress relaxation, retardation) are used. The short-term, however, is dominated by dynamic test methods with oscillating loading that fall into the category of dynamic–mechanical analysis. Relationships between statically and dynamically determined values can be established on the basis of linear viscoelasticity theory [1.16, 4.12].

4.2.1.1 Static Testing Methods

Static testing methods are based on the analysis of material behavior subsequent to a sudden change in mechanical loading. We can make a principal distinction between two cases as illustrated by the diagrams in Fig. 4.9.

In stress relaxation (Fig. 4.9a), the change of stress with time $\sigma(t)$ at $\varepsilon_0 = const.$ caused by a sudden change in deformation is measured. From this we obtain the material parameter called time-dependent modulus of elasticity $E(t)$:

$$E(t) = \frac{\sigma(t)}{\varepsilon_0} \tag{4.50}$$

By analogy in the retardation or creep test (Fig. 4.9b), the change of deformation $\varepsilon(t)$ with time to the value $\sigma_0 = const.$ as a result of a sudden change in stress is used to determine compliance value $C(t)$:

$$C(t) = \frac{\varepsilon(t)}{\sigma_0} \tag{4.51}$$

Static tests can extend over very long time periods. They therefore place strong demands on the constancy of test conditions, especially temperature and humidity. In addition, structural changes such as chemical reactions and physical ageing can influence material behavior. During relatively short loading times, experimental results are influenced by the loading velocity.

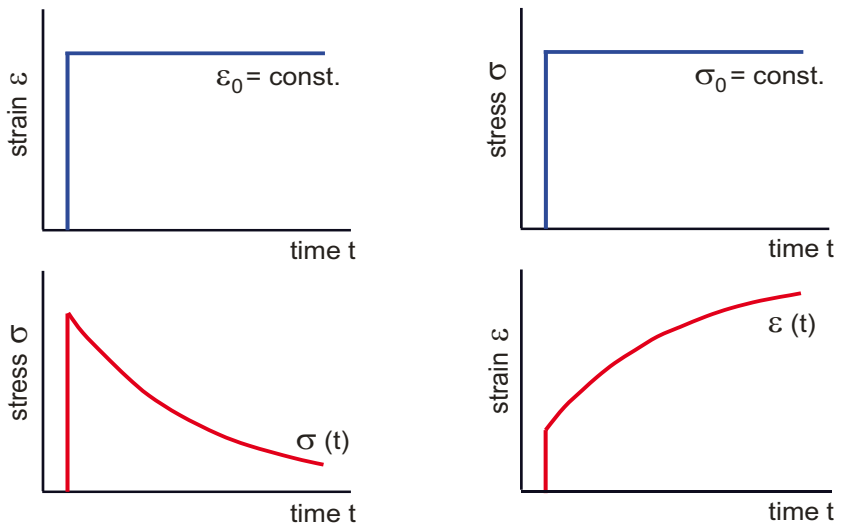

Fig. 4.9: Stress relaxation and retardation (creep) for characterizing viscoelastic behavior at long loading times

4.2.1.2 Dynamic–Mechanical Analysis (DMA)

In dynamic–mechanical analysis, specimens are subjected to oscillating loading. The time dependence of material behavior can be characterized by varying the frequency. For the relation between loading time t and frequency f or angular frequency ω, the rule is:

$$t = \frac{1}{2\pi f} = \frac{1}{\omega} \tag{4.52}$$

DMA is especially useful since only relatively short test times are required to acquire viscoelastic values over a wide frequency range. Moreover, dynamic–mechanical–thermal analysis (DMTA) makes it relatively easy to investigate material behavior as a function of temperature.

A number of procedures are available for performing DMA that differ with respect to the achievable frequency range, type of mechanical loading and magnitude of measurable material properties. These procedures can be classified according to the type of vibrational excitation, such as forced vibrations, freely damped vibrations and resonant vibrations. In higher frequency ranges, the propagation of sonic and ultrasonic waves is also used to determine characteristic values. The various methods of DMA are standardized by ISO 6721.

Tests Using Forced Vibrations

When forced vibrations are used to characterize viscoelastic properties, specimens are subjected to sinusoidal alternating mechanical loading at constant frequency and constant amplitude. In cases of linear-viscoelastic material behavior, steady-state changes of stress and deformation with time exhibit the same frequency, but varying phase positions. For cases of normal stress loading, the rule is:

$$\varepsilon(t) = \varepsilon_0 \sin \omega t \tag{4.53}$$

$$\sigma(t) = \sigma_0 \sin(\omega t + \delta) \tag{4.54}$$

This is illustrated in Fig. 4.10.

Due to the phase shift δ between stress and strain, its modulus has to be introduced as the complex modulus E^* to describe the stress–strain relationship.

$$E^* = E' + iE'' \tag{4.55}$$

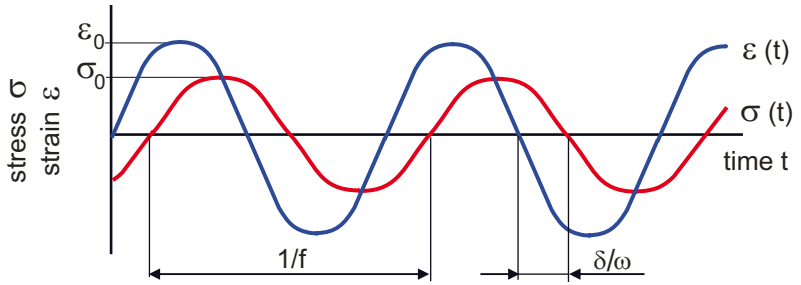

Fig. 4.10: Change in stress and strain with time in dynamic–mechanical analysis using forced vibrations

This complex modulus can be regarded as a vector in the complex plane (Fig. 4.11) whose direction is given by the phase angle δ and its amount by the ratio of stress and strain amplitudes:

$$\left|E^*\right| = \frac{\sigma_0}{\varepsilon_0} \tag{4.56}$$

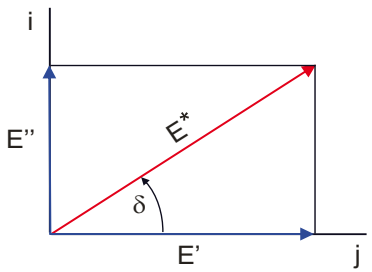

Fig. 4.11: Diagram of modulus E* in the complex plane

Using simple trigonometric relations, a real part E' and an imaginary part E'' can be distinguished:

$$E' = E^* \cos\delta = \frac{\sigma_0}{\varepsilon_0}\cos\delta \qquad \text{and} \tag{4.57}$$

$$E'' = E^* \sin\delta = \frac{\sigma_0}{\varepsilon_0}\sin\delta \tag{4.58}$$

The real part E' is called the storage modulus. It is a measure of the energy storable during the oscillation period W_{rev}. By contrast, the imaginary part E'' of the complex modulus is related to the energy dissipated during the oscillation period W_{irrev}. For this reason, it is called the loss modulus.

$$W_{rev} = \frac{1}{2}E'\varepsilon_0^2 \tag{4.59}$$

$$W_{irrev} = \pi E'' \varepsilon_0^2 \tag{4.60}$$

From the ratio of loss and storage moduli, we obtain the loss factor $\tan \delta$ that characterizes the damping behavior of the material:

$$\tan \delta = \frac{E''}{E'} = \frac{1}{2\pi} \cdot \frac{W_{irrev}}{W_{rev}} \tag{4.61}$$

The forced vibration procedure is limited to frequencies below specimen resonance frequency. Commercial devices have a range of approx. 10^{-2} Hz to 10^{2} Hz. Measurement can be controlled by monitoring both strain and stress, thus enabling the determination of complex modulus E^* and complex compliance C^*. Using axial and torsional testing equipment and an appropriate specimen adapter, various loading types (tensile, compression, bending, shear, torsion) can be employed. This enables the acquisition of complex elasticity and shear moduli over a wide stiffness range from 10^{-3} MPa to 10^{6} MPa. The most significant disadvantage of this procedure lies in its lack of sensitivity when measuring relatively low damping ($\tan \delta < 0.01$).

Thanks to their wide application range, test methods with forced vibrations play a dominant role in the dynamic–mechanical analysis of polymer materials.

Tests Using Free Damped Vibrations (Torsion Pendulum)

When a specimen is deflected from its state of equilibrium by pulsed deformation, it returns to its state of equilibrium in free damped vibrations. The natural frequency of vibration, as well as the decrease of vibration amplitudes with time, depends on the viscoelastic properties of the material.

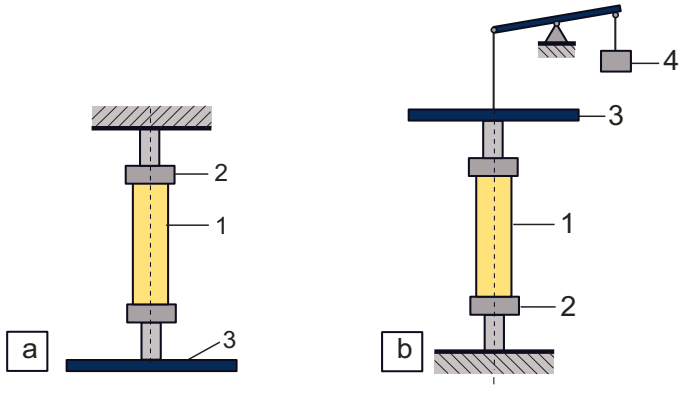

Fig. 4.12: Diagram of a torsion pendulum setup without counterweighting (a) and with counterweighting (b)

The principle of free damped vibrations has its practical application in torsion pendulum testing as standardized in ISO 6721-2. The basic setup of the torsion pendulum is illustrated in Fig. 4.12.

Usually a prismatic specimen (1) is firmly clamped at one end (2). At the other end it is connected to an oscillating weight (3) that influences the moment of inertia and thereby the eigenfrequency of the entire system. In order to eliminate longitudinal normal stresses in the specimen, a counterweight (4) can be applied. The specimen is excited to freely decreasing torsional oscillations by pulsed deformation of the oscillating weight as shown in Fig. 4.13.

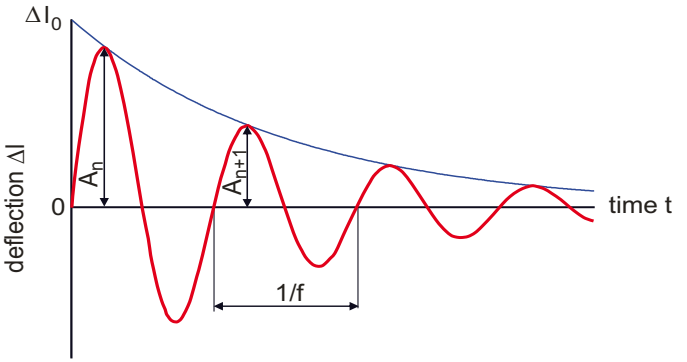

Fig. 4.13: Freely decaying damped vibration

The storage modulus G' can be determined from vibration eigenfrequency. According to ISO 6721-2:

$$G' = 4\pi I\left(f_d^2 F_d - f_0^2\right) F_g \tag{4.62}$$

Here f_d is the eigenfrequency of the pendulum with, and f_0 the eigenfrequency of the pendulum without the specimen (if work without counterweighting, then $f_0 = 0$). Additional influencing factors to be considered include the moment of inertia I of the oscillation weight with clamping, as well as the damping correction F_d and the geometry factor F_g. When prismatic specimens are used (clamping length L, width b, thickness h), with $h/b \leq 6$ and a geometry correction factor $F_c = 1 - 0.63\ h/b$, then:

$$G' = 12\pi^2 I f_d^2 \left(1 - (\Lambda/2\pi)^2 - (f_0/f_d)^2\right) L/\left(bh^3 F_c\right) \tag{4.63}$$

The logarithmic decrement Λ characterizes system damping. It is determined from the ratio of sequential vibration amplitudes:

$$\Lambda = \ln \frac{A_n}{A_{n+1}} \tag{4.64}$$

Using logarithmic decrement, the loss modulus G'' can be calculated as

$$G'' = 4\pi I f_d^2 \left(\Lambda - \Lambda_0\right) F_g \tag{4.65}$$

For work without counterweighting, the logarithmic decrement of the pendulum without specimen Λ_0 is 0. For specimens with square cross-sections and small h/b ratio and with counterweighting at low internal damping of the pendulum ($\Lambda_0 << \Lambda$), the loss modulus can be calculated as:

$$G'' = 12\pi I f_d^2 \Lambda L \Big/ \left(b h^3 F_c\right) \tag{4.66}$$

With the storage and loss moduli, the complex modulus G^* and the loss factor tan δ can be determined analogous to Eqs. 4.57, 4.58 and 4.61.

The torsion pendulum works at frequencies ranging from 0.1 to 10 Hz. It is preferred for investigating materials with low damping (tan $\delta \leq 0.1$). When investigating with temperature dependence, a change takes place in system eigenfrequency due to modulus changes (see, e.g., Eq. 4.62). Modulus temperature curves are therefore generally measured at sliding frequency. To be sure, the frequency changes can be compensated in principle via changes in the moment of inertia of the oscillating weight. Basic advantages of the torsion pendulum are the simplicity of its setup and measurement, as well as its high level of sensitivity.

Tests Using Forced Resonant Oscillation

When forced oscillations are generated at a frequency whose wave length approaches the dimensions of the specimen, resonant phenomena occur. If the specimen is excited in the range of resonance at constant force amplitude, the amplitude of deflection follows a peaked curve (Fig. 4.14). Resonant frequency f_i and width at half maximum Δf_i are related to the viscoelastic properties of the material being investigated.

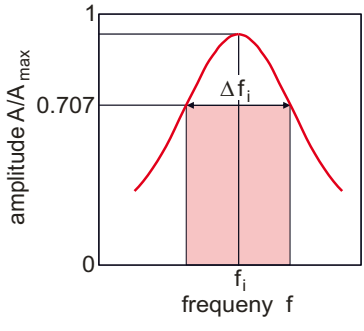

Fig. 4.14: Resonance curve of a viscoelastic material

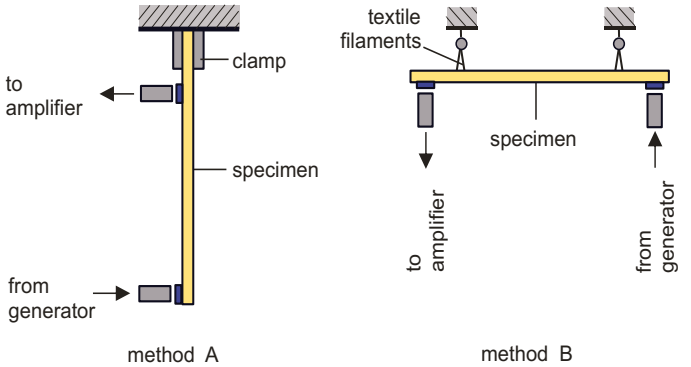

Fig. 4.15: Test setup for acquiring viscoelastic properties with forced resonant oscillation

Forced resonant oscillations are applied to determine the complex modulus by the flexural vibration-resonance-curve method (ISO 6721-3). A prismatic rod is used as specimen and clamped either on one side (procedure A) or hung on textile fibers at the vibration nodes (procedure B). The diagram in Fig. 4.15 illustrates both arrangements. Non-contacting excitation and measurement are performed via electromagnetic transducers connected to the polymer material via thin metal tabs glued to the specimen surface. Using a frequency synthesizer, the excitation frequency can be continuously varied over a range from approx. 10^1 Hz to 10^3 Hz.

While scanning this frequency range, the detector registers several peaks in oscillation amplitude corresponding to different order resonances i (i = 1, 2, 3,…). The real part of the complex elasticity modulus E' can be determined from resonance frequency f_i at the i-th resonance point, density ρ of the investigated material and specimen dimensions (free length L, thickness h):

$$E' = \left(4\pi\sqrt{3\rho}\,\frac{L^2}{h}\right)^2 \left(\frac{f_i}{k_i^2}\right) \tag{4.67}$$

The numerical value k_i^2 depends on the order number i of the resonance point and clamping conditions (see Table 4.1).

Table 4.1: Numerical value k_i^2 for determining storage modulus E′ with the flexural vibration test

Order number i	k_i^2 (Method A)	k_i^2 (Method B)
1	3.52	22.4
2	22.0	61.7
> 2	$(i-1/2)^2\pi^2$	$(i-1/2)^2\pi^2$

The additional parameter loss factor tan δ can be calculated from the width at half-maximum of resonance curve Δf_i and resonance frequency f_i:

$$\tan\delta = \frac{\Delta f_i}{f_i} \tag{4.68}$$

For materials with low internal damping (tan $\delta < 0.01$) and resonance frequency, the analysis of freely decreasing vibrations after the exciter has been shut off can be recommended as an alternative. Here, the falling amplitudes of sequential vibrations is observed (see Fig. 4.13), from which the loss factor can be determined using the logarithmic decrement Λ:

$$\tan\delta = \frac{\Lambda}{\pi} = \frac{1}{\pi}\ln\frac{A_n}{A_{n+1}} \tag{4.69}$$

The flexural vibration test is especially suited for characterizing rigid materials whose loss factor does not significantly exceed the value tan $\delta = 0.1$. A decisive disadvantage of this procedure lies in the fact that relatively few resonance points are available and that the position of resonance points can be influenced only by altering specimen dimensions. During temperature-dependent measurements, changes take place in resonance frequency so that it is impossible to acquire values at constant frequency. Based on the achievable frequency range, the characterization of structure-borne sound insulating materials is the preferred application area for flexural vibration tests.

Tests Based on Wave Propagation (Ultrasonic Technique)

Above resonance frequency, the wave length of oscillating mechanical loading is short compared to specimen dimensions. That makes it possible to use the wave propagation characteristic of a material to determine its viscoelastic properties. Such investigations are generally performed using an ultrasonic ($f > 20$ kHz) pulse-echo or pulse-transmission technique [4.29, 4.30]. Sound velocity v and sound absorption coefficient α are obtained from acoustic path length l and the corresponding pulse transit time, as well as from pulse amplitudes I_1 and I_2 at various path lengths l_1 and l_2.

$$v = \frac{l}{t} \tag{4.70}$$

$$\alpha = \frac{1}{l_2 - l_1}\ln\frac{I_1}{I_2} \tag{4.71}$$

When the density ρ of the material is known, longitudinal wave modulus L and shear modulus G can be determined using longitudinal waves (v_l, α_l) and transverse waves (v_t, α_t) respectively. At low damping ($\alpha\lambda/2\pi << 1$), we can approximate that [4.31]:

$$L' = \rho v_l^2 \quad \text{and} \quad L'' = \frac{2\rho\alpha_l v_l^3}{\omega} \tag{4.72}$$

$$G' = \rho v_t^2 \quad \text{and} \quad G'' = \frac{2\rho\alpha_t v_t^3}{\omega} \tag{4.73}$$

According to elasticity theory, the modulus of elasticity E' can be calculated from longitudinal wave modulus and shear modulus. It depends on the ratio of propagation velocities of transverse and longitudinal waves:

$$E' = \frac{3L' - 4G'}{L'/G' - 1} = 4\rho v_t^2 \cdot \left(\frac{0.75 - (v_t/v_l)^2}{1 - (v_t/v_l)^2} \right) \tag{4.74}$$

Ultrasonic methods have gained great importance for determining the properties of oriented polymers and polymer composites. All components of the stiffness matrix can be acquired from a single specimen by varying the polarization direction and propagation direction of the ultrasonic waves.

Ultrasonic measurements are typically made at frequencies between 100 kHz and 100 MHz. The top end of the frequency range is defined by the strong increase in damping. Various vibration exciters have to be used when working in this wide frequency range. Relatively large frequency ranges can be covered following broadband excitation by applying *Fourier* analysis [4.32].

4.2.2 Time and Temperature Dependence of Viscoelastic Properties

The time and temperature dependence of viscoelastic properties is quite significant for polymer material engineering. That is why it provides the basis for classification into elastomers, thermoplastic elastomers, thermoplastics and thermosets. The diagram in Fig. 4.16 illustrates the dependence of the viscoelastic properties storage modulus E', loss modulus E'' and loss factor tan δ on loading time t for an amorphous thermoplastic.

Based on the discontinuous curve of the storage modulus E', viscoelastic behavior can be divided into four characteristic regions. Under short-term loading ($t << \tau_\alpha$), the material exists in its glassy state. Here, at values between 10^9 Pa and 10^{10} Pa, the storage modulus is only slightly time-dependent. In the glass transition region

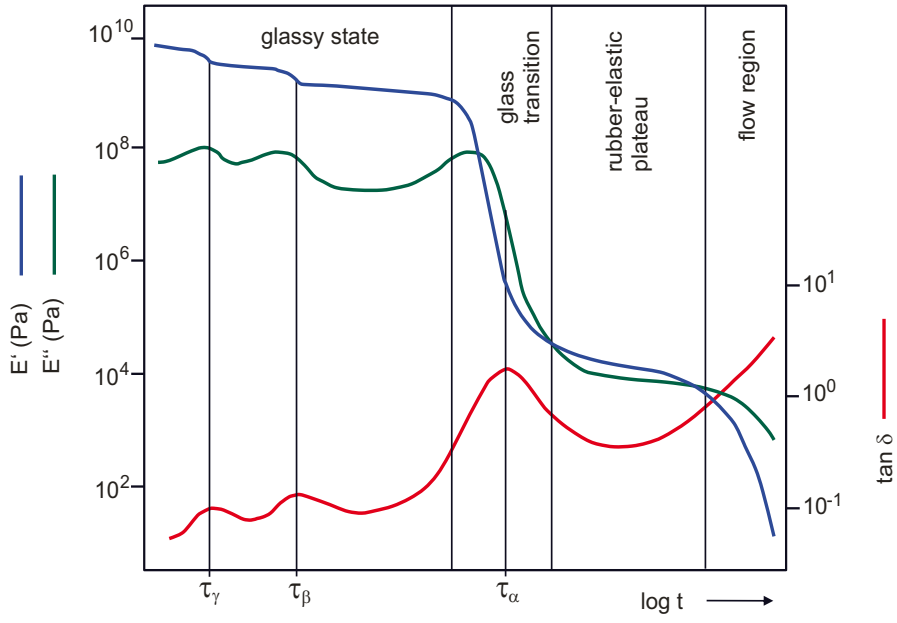

Fig. 4.16: Time dependence of viscoelastic properties of an amorphous thermoplastic

($t \approx \tau_\alpha$), a drastic reduction of the storage modulus by 3 to 4 decades occurs over a relatively short time span. This is followed by a more or less pronounced rubber-elastic plateau where the material is soft and deformable like rubber. At very long loading times, viscous properties dominate mechanical behavior in the flow region.

The time dependence of the storage modulus is calculated according to Eq. 4.35 using a relaxation time spectrum $H(\tau)$ whose structural cause is a spectrum of molecular relaxation processes. The discontinuous changes in curve shape are due to changes in the dominant relaxation mechanism. At the same time, the mechanical losses (E'', tan δ) pass through a local maximum due to molecular friction.

The most significant relaxation process in amorphous thermoplastics is the glass transition, also called primary relaxation or α process. It is related to the activation of micro *Browninan* motion. By this we mean cooperative rearrangements of rather long sections of polymer chains (approx. 50 to 100 CH_2 units). In the glassy state of amorphous polymers, additional secondary relaxation processes (β, γ process) can occur that are caused by molecular motion of substituents, side chains, or short mainchain segments. A simultaneous increase in relaxation time can generally be observed that is on the order of the structural units partaking in the relaxation process. Secondary relaxation processes have relatively little influence on the storage modulus E' of the material; however, they can effect sometimes distinct partial change in toughness [4.33].

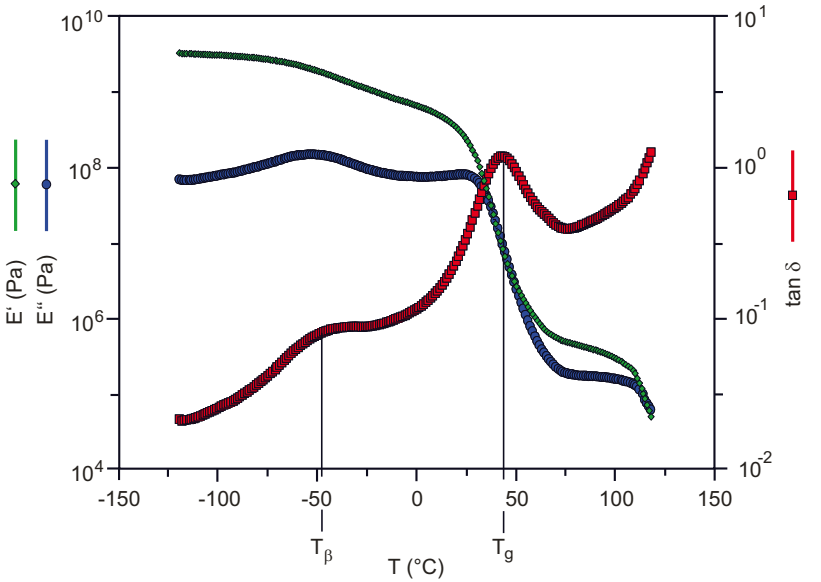

Fig. 4.17: Modulus–temperature curves and mechanical loss factor dependent on temperature for polyvinylbutyrate (frequency f = 1 Hz)

After passing through the glass transition region, entropy elasticity (see Section 4.1.2.1) dominates mechanical behavior in the rubber-elastic plateau. In this region, entanglements act as temporary crosslinks in a flexible-chained polymer network. Disentanglement processes lead, after very long loading times, to a loosening of the network crosslinks. Thereby, irreversible flow processes are enabled.

The changes in viscoelastic properties presented in Fig. 4.16 take place in amorphous thermoplastics over a time span of 15 to 20 decades. Since this large area can only be partially covered experimentally, investigations to characterize viscoelastic behavior are often performed on the basis of temperature dependence. According to the time–temperature equivalence (see Section 4.1.2.3), it is possible to acquire the entire spectrum of viscoelastic properties at constant loading time or frequency in one temperature run. As a result of such measurements, Fig. 4.17 shows the temperature dependence of storage modulus E', loss modulus E'', as well as loss factor tan δ for amorphous thermoplastic polyvinylbutyrate. The tests were performed at 1 Hz constant frequency under dynamic tensile loading in the range of $-120\ °C \leq T \leq +120\ °C$. Glassy state, glass transition, rubber-elastic plateau and flow region can be clearly distinguished. The dynamic glass transition temperature T_g is an important engineering parameter and can be determined in practice by the maximum of the loss factor. However, the peak of the storage modulus shifted to lower temperatures is sometimes used as a reference point. In contrast to the results of static testing methods (calorimetry, dilatometry), glass temperature under dynamic loading

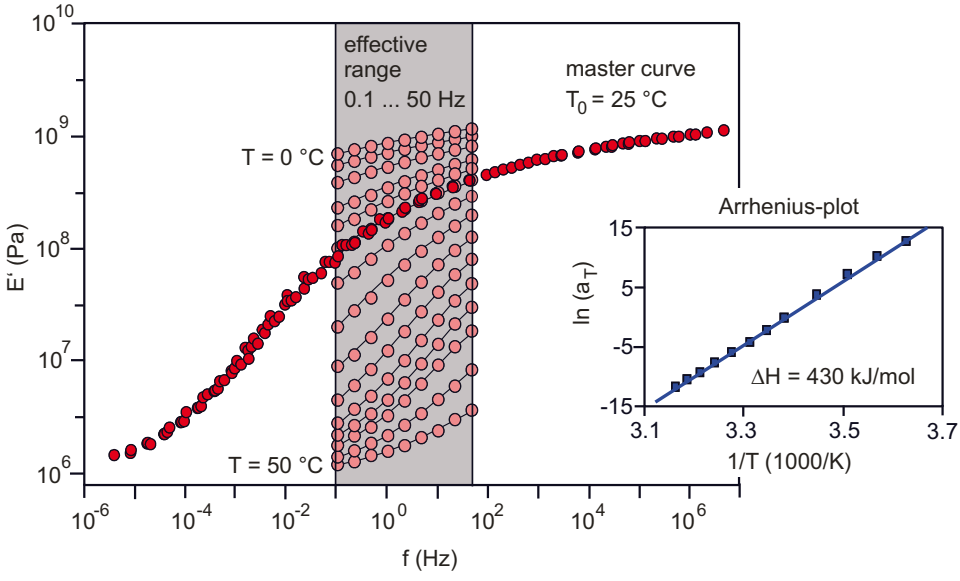

Fig. 4.18: Master curve of the storage modulus of polyvinylbutyrate for reference temperature $T_0 = 25$ °C

is generally observed at higher temperatures due to the time dependence of viscoelastic properties.

If temperature-dependent measurements of viscoelastic properties are performed at various frequencies, a master curve can be constructed using the time-temperature superpositon principle (see Section 4.1.2.3) that provides for an estimation of viscoelastic behavior beyond the experimentally covered time period for a reference temperature T_0. Such a master curve is illustrated in Fig. 4.18.

Based on experimental data acquired at temperatures from 0 °C to 50 °C over a frequency range of 0.1 Hz to 50 Hz (effective range) in the glass transition range, mechanical behavior can be estimated over a time span of more than 10 decades.

4.2.3 Structural Factors Influencing Viscoelastic Properties

Relationships between chemical structure, molecular relaxation processes and viscoelastic properties are of great practical interest for characterizing and developing materials. That is why they are the object of intensive theoretical [4.34, 4.35] and experimental studies [4.36 – 4.38].

From the time and temperature dependence of the viscoelastic properties of amorphous polymers, information can be acquired as to their chain stiffness (chemical structure of backbone chains and substituents), molecular interactions

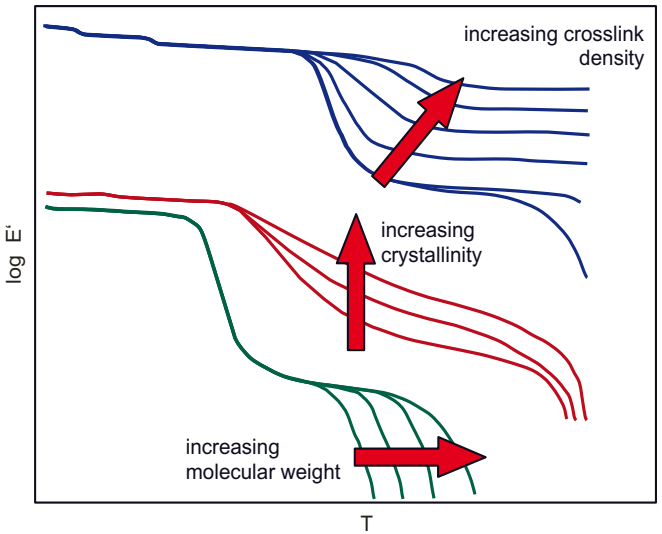

Fig. 4.19: Influence of molecular weight, crosslink density and degree of crystallinity on the temperature dependence of storage modulus

(molecular coefficient of friction), molecular weight and molecular weight distribution, crosslink density and molecular orientation, among others. For semicrystalline polymers, statements can be made as to the degree of crystallinity and crystallite morphology (lamellar thickness). Viscoelastic properties also have great significance for investigating the composition, phase morphology and interface effects of copolymers and polymer blends. Figure 4.19 illustrates the influence of molecular weight, crosslink density and degree of crystallinity on the temperature dependence of storage modulus.

Figure 4.20 illustrates the differences in temperature dependence of the viscoelastic properties of homogenous and heterogeneous polymer systems based on styrene–butadiene copolymers. The two-phase block copolymer (SBS) exhibits two separate glass transitions in the transition temperature regions of the base components polybutene (PB) and polystyrene (PS). However, only one glass transition is detected in the single phase statistical copolymer (SBR) whose temperature position, corresponding to the composition of the mixed phase, is shifted relative to the values of its base components.

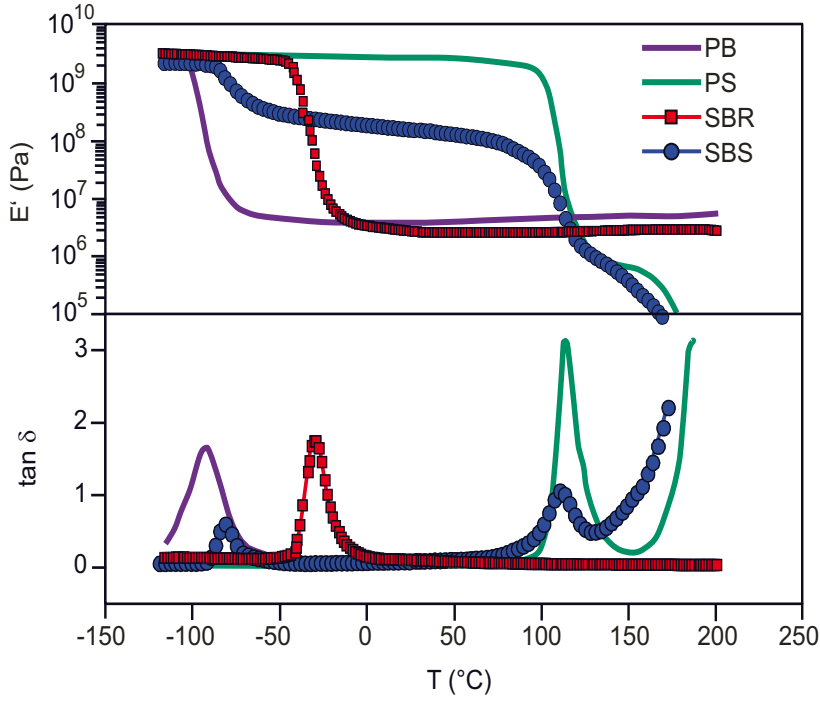

Fig. 4.20: Comparison of temperature dependence of storage modulus and loss factor of homogenous (SBR) and heterogenous (SBS) styrene–butadiene copolymers with the corresponding homopolymers (PB and PS)

4.3 Quasi-Static Test Methods

4.3.1 Deformation Behavior of Polymers

By quasi-static test methods, we mean mechanical tests involving strain rates ranging from approx. 10^{-5} to 10^{-1} s^{-1} in which specimen fracture or a predetermined load limit is reached in an economically reasonable time span. It is thereby assumed that loading proceeds slowly, impact-free and increases continuously to fracture. Thus, universal test machines employed in such tests must ensure that the cross-head speed remains constant, regardless of load level and loading speed, when using the preferred conventional test methods. Under these formal conditions, quasi-static test methods such as tensile or flexural tests mainly serve to acquire material values or material characteristic functions. They are also applied in quality assurance, failure analysis and pre-selection of polymers for specified applications, as well as for solving simple design problems [1.38].

The total deformation of mechanically loaded polymers has the following components, whereby the absolute amount of such components depends on effective loading time and acting temperature:

- elastic deformation,
- linear-viscoelastic deformation,
- non-linear viscoelastic deformation and
- plastic deformation.

In unreinforced plastics, the region of elastic deformation, which corresponds to changes in atomic distance and valency angle in the macromolecule while simultaneously storing elastic potential energy, is typically very small . The molecular links generated in the production process are not released in cases of energy-elastic deformation. In such materials, this region corresponds to a reversible strain of < 0.1 % and, given a linear relation between stress and strain, is completely described by *Hooke*'s law. In thermosets with network structures or highly filled or reinforced thermoplastic materials, this behavior can be detected especially at short loading times and/or low temperatures up to 40 % of the corresponding stress at break [4.39]. Especially in unidirectional reinforced fiber composites, this deformation behavior is dominant up to break of the specimen used.

Other than in metallic materials, polymers exhibit a mechanically reversible, but time-dependent deformation behavior (viscoelasticity), even on small deformations and at temperatures dictated by application. Based on load level, a principle distinction is made between the linear-viscoelastic and the non-linear viscoelastic deformation component (see Section 4.1.2.3).

Linear-viscoelastic deformation is characterized by mechanically stimulated molecular rearranging processes in which the existing molecular links are not released. This deformation region in thermoplastic polymers lies empirically in an interval between 0.1 and approx. 0.5 % of the total applied strain and passes over into non-linear viscoelastic deformation. The strain occuring as a reaction to loading is reversible, but time- and temperature-dependent, as the diagrams in Fig. 4.21a, b show for static loading. During loading and unloading, it amounts to less than the applied stress. A hysteresis curve (Fig. 4.21c) is created whereby, in cases of quasi-static loading, special initial effects can result, such as zero drift or stress relaxation [4.40].

We define *non-linear viscoelastic deformation behavior* with the release of molecular entanglements when the polymer properties depend not only on time and temperature, but also on the level of mechanical load. In this deformation region, which is characterized by the beginning of microstructural material damage, molecular migrations take place leading to irreversible yield processes and thereby to

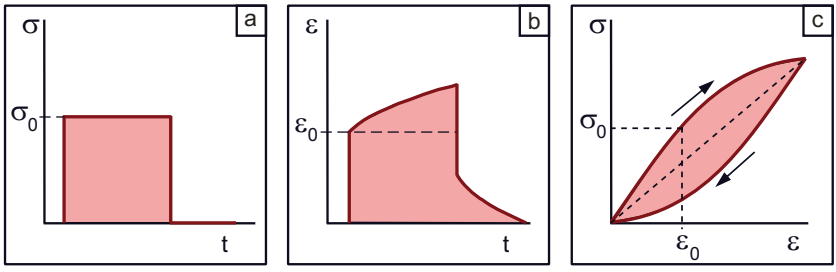

Fig. 4.21: Linear-viscoelastic deformation behavior of polymers in a diagram illustration of stress-time function (a) and strain-time function (b) given static as well as stress–strain function c) under quasi-static loading

permanent deformation [4.41]. The plastic deformation of polymer products is often mentioned in connection with "cold" yielding and stretching and hardening processes. The polymers then often exhibit clearly definable yield stresses depending on the type of loading selected, as well as on testing speed and temperature. Depending on the mentioned factors and the type of polymer, the dominant deformation mechanisms are crazes and shear band formation, both demonstrable using microstructural investigation methods [4.42], but which are sometimes even macroscopically visible as well.

The great variety of polymers created by chemical modification, mixing, filling and reinforcing leads, due to interaction among the various organic and inorganic components, to new internal top or border surfaces from which numerous different damage mechanisms may result. These mechanisms, such as fiber breaking or debonding, as well as the formation of voids and microcracks, begin to act immediately in the transition range between linear- and non-linear viscoelastic deformation and affect the durability and reliability of such materials in use. Here the problem arises that such effects are not visible on the stress–strain diagram. Therefore, they can only be demonstrated indirectly via stiffness loss in the specimen employed, or using one the hybrid methods of polymer diagnostics (cf. Chapter 9).

Regardless of the deformation behavior described and the occurring damage mechanisms, the production related internal state of the specimen employed has a decisive effect on stress– deformation behavior. Due to their incomparable residual stresses and orientations, specimens produced by different manufacturing methods (e.g. compression and injection molding) have to be considered component parts. That means that molding material properties can only be determined under idealized conditions (cf. Chapter 2). Based on the test conditions in quasi-static test methods, varying residual stresses and orientations affect the E modulus, while varying orientation states especially influence strength and deformation behavior.

Values acquired by quasi-static test methods are influenced by retardation and/or relaxation behavior overlaying the mechanical experiment, as well as by the particular specimen state, test conditions and any occurring damage mechanisms. When the stress–strain behavior of a hypothetical polymer without the influence of time is considered under this aspect in the tensile test, a stress–strain curve results such as the one presented Fig. 4.22a. If, in the experiment, influence from retardation mechanisms occurs, strain increases due to simultaneously occurring creep (Fig. 4.22b). If in addition, relaxation mechanisms are active, strain at break remains constant, but tensile strength is significantly reduced (Fig. 4.22c). In actual tensile tests, both components occur simultaneously, thus influencing strength, E modulus and deformation (Fig. 4.22d).

Any variation in test conditions regarding temperature and cross-head speed v_T (1 to 500 mm min^{-1}), as is sometimes permitted in the common test specifications, leads to a wide spectrum of material values. The occurring relaxation and creep processes over the range of practically relevant temperatures and application times cannot be ignored when dimensioning plastic components and testing polymers. In thermosets and thermoplastics used for design purposes in the glassy state, the real loads do not

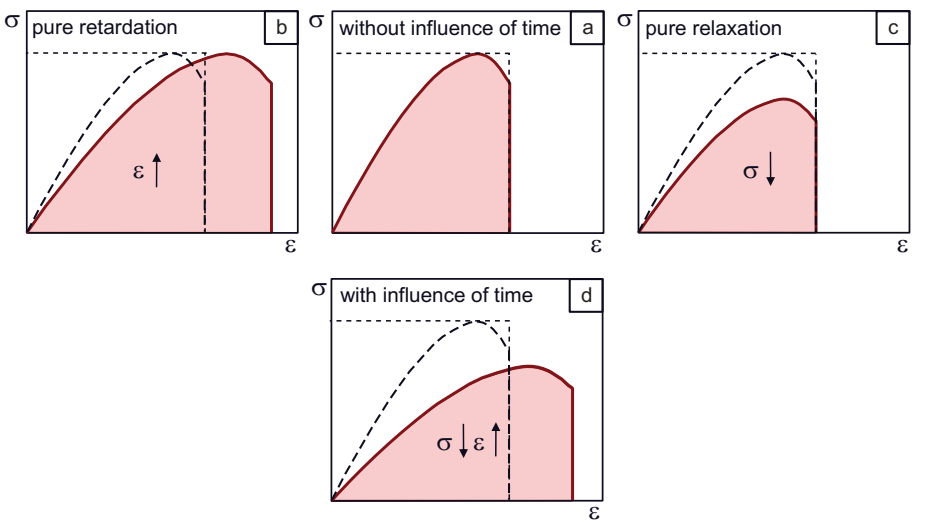

Fig. 4.22: Diagram of the stress–strain behavior under quasi-static loading without time influence (a), with retardation influence (b), with stress relaxation influence (c) and with time influences (d)

usually lie in the immediate neighborhood of the transition regions. Thus, for these materials, defined E modulus values can be given that depend very little on loading time and temperature. However, for many thermoplastic polymers the temperature range of their engineering application is within their transition ranges, thus strongly

involving dependence of the material values acquired on loading time, ambient temperature and load level (Fig. 4.23). For selected thermoplastic polymers, Fig. 4.23 shows the relationship between the E modulus E_t acquired by tensile test, loading time t and test temperature T. Here, an obvious impact on value levels is being measured dependent on the type of polymer and its corresponding transition ranges that can significantly limit the material's area of application.

The behavior illustrated in Fig. 4.23 can be permanently influenced by adding fillers or reinforcers such as chalk, talc, carbon or glass-fibers [4.43], as well as nanoparticles [4.44].

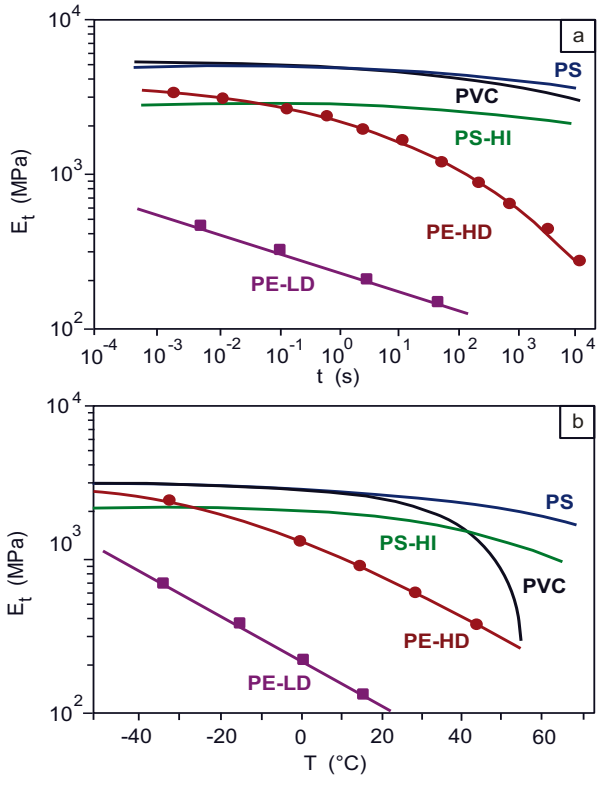

Fig. 4.23: E modulus acquired by tensile test for selected polymers as a function of time (a) and temperature (b)

As can be clearly seen from the functional relationships illustrated, the strength and stiffness behavior of polymers cannot be described by single-point data. These are acceptable only when the test conditions are univocal and reproducible. As a matter of principle, the mechanical values of polymers should be acquired on the basis of time and temperature dependence and be described by functional relationships. In summary, it can be said that every value measured for polymers is influenced by a

series of factors determined by measurement and test techniques, as well as by the production of test specimens:

- State and properties (M) of the molding material to be tested, such as chemical structure, viscosity, molecular weight and its distribution, as well as fillers and reinforcers employed,
- The process used to produce the specimen and the resulting internal state (S) in the specimen such as morphology, residual stresses, orientation and degree of crystallinity,
- Specimen geometry (G), such as on dumbell specimens or flat specimens, notch stress, dynamic and static weld lines, as well as structural inhomogeneities, such as cavities or agglomerates, and
- Test strategy and test technique that can be subsumed in the concept of test conditions (T), i.e., type of loading, testing temperature and testing velocity, as well as ambient influences (moisture, UV radiation, etc.).

Consequently, any property P measured on a specimen is a function of the parameters listed above:

$$P = f(M, S, G, T) \tag{4.75}$$

Characteristic values can only be measured reproducibly, if these relationships are known and appropriately considered. That means that the prerequisites for reproducible measurements include comparable chemical and physical structure and morphology, as well as identical geometric conditions and identical test methodology.

General tendencies can be stated for the relationship between strength and deformation behavior and internal state:

- Polymer strength increases, for example, with increasing molecular weight, increasing degree of crosslinking, increased orientation or by filling or reinforcing the polymer whereby deformation behavior is generally reduced;
- Strength is reduced by increased moisture, increasing age, degradation or decomposition; by contrast, deformability can increase or decrease depending on various deformation processes.

However, these statements are specific to the material and not generally valid, as for example is shown by positive post-crystallization effects due to ageing.

Based on the relations illustrated between structure and properties, it is clear that values acquired on standardized specimens cannot be carried over directly to plastics components.

The most important – and in practice most significant – mechanical tests are the tensile test, bend test and compression test, as well as the tear test relevant for foils. Torsional testing, however, bears little relevance for polymers. In addition to these basic tests, there are various test methods based on comparable measurement technology. They serve especially to characterize joints (glued and welded lines), and to determine adhesive strength and interlaminar shear strength. They include the shear tension or shear bend and the peel test [4.46] (see Chapter 10).